

# An epidemic model for COVID-19 transmission in Argentina: Exploration of the alternating quarantine and massive testing strategies

Lautaro Vassallo<sup>1,2\*</sup>, Ignacio A. Perez<sup>1,2</sup>, Lucila G. Alvarez-Zuzek<sup>3</sup>, Julián Amaya<sup>2</sup>, Marcos F. Torres<sup>1,2</sup>, Lucas D. Valdez<sup>1,2</sup>, Cristian E. La Rocca<sup>1,2</sup>, Lidia A. Braunstein<sup>1,2</sup>

**1** Instituto de Investigaciones Físicas de Mar del Plata (IFIMAR), CONICET -  
Universidad Nacional de Mar del Plata, 7600 Mar del Plata, Buenos Aires, Argentina

**2** Departamento de Física, Facultad de Ciencias Exactas y Naturales, Universidad Nacional  
de Mar del Plata, 7600 Mar del Plata, Buenos Aires, Argentina

**3** Department of Biology, Georgetown University, Washington, D.C. 20057, United States

\* lvassallo@mdp.edu.ar

## Abstract

The COVID-19 pandemic has challenged authorities at different levels of government administration around the globe. When faced with diseases of this severity, it is useful for the authorities to have prediction tools to estimate in advance the impact on the health system and the human, material, and economic resources that will be necessary. In this paper, we construct an extended Susceptible-Exposed-Infected-Recovered model that incorporates the social structure of Mar del Plata, the 4<sup>o</sup> most inhabited city in Argentina and head of the Municipality of General Pueyrredón. Moreover, we consider detailed partitions of infected individuals according to the illness severity, as well as data of local health resources, to bring these predictions closer to the local reality. Tuning the

corresponding epidemic parameters for COVID-19, we study an alternating quarantine strategy, in which a part of the population can circulate without restrictions at any time, while the rest is equally divided into two groups and goes on successive periods of normal activity and lockdown, each one with a duration of  $\tau$  days. Besides, we implement a random testing strategy over the population. We found that  $\tau = 7$  is a good choice for the quarantine strategy since it matches with the weekly cycle as it reduces the infected population. Focusing on the health system, projecting from the situation as of September 30, we foresee a difficulty to avoid saturation of ICU, given the extremely low levels of mobility that would be required. In the worst case, our model estimates that four thousand deaths would occur, of which 30% could be avoided with proper medical attention. Nonetheless, we found that aggressive testing would allow an increase in the percentage of people that can circulate without restrictions, being the equipment required to deal with the additional critical patients relatively low.

## 1 Introduction

In March 2020 the World Health Organization (WHO) officially announced the COVID-19 (disease caused by the novel SARS-CoV-2 coronavirus) as a pandemic. The world was about to witness one of the most devastating pandemics in last decades. In December 2019, a cluster of a novel pneumonia-like illness was identified in Wuhan (China) and, without the proper control measures, in 3 months the disease rapidly spread all over the world. The first stages of the propagation occurred in different countries of Europe, leading to countless human life losses and a severe economic crisis.

On March 3, the first COVID-19 patient was confirmed in Buenos Aires, Argentina. It was an imported case, a 43-year-old man who had arrived from Milan, Italy. Following international protocols and recommendations of local experts, educational centers of all levels

were closed, massive shows were suspended and international frontiers were closed. Decisively, on March 19 and in order to restrict the spread of the new coronavirus, the national government announced a 12 days nationwide lockdown for all citizens in the country [1]. These measures were extended progressively until nowadays with certain relaxations. Until the middle of September, the total number of confirmed cases surpassed 750 thousand and the number of fatalities was around 17 thousand, most of them concentrated in the Capital Federal (CABA) and the suburbs, which form the urban conglomerate denoted by AMBA, inhabited by 37% of the total population in Argentina.

Researchers have put a lot of effort in the study of multiple aspects of COVID-19 pandemic in several countries [2–6], at country level and at big regions with a high concentration of people [7]. For instance, Romero *et al* [8] simulated an agent-based model for COVID-19 in Argentina. The authors analyzed the evolution of four different pandemic scenarios, with different levels of restriction in population mobility, and they found that social isolation is the measure that has more impact in the spread of the virus. In the same way, in [9], researchers found that early school closures effectively helped in reducing the mortality rate in Argentina, Italy and South Korea. For its part, Torrente *et al* [10] showed the psychological impacts of the pandemic and early measures implemented, in the form of substantial anxious and depressive symptoms. Moreover, Quirós *et al* [11] conducted a seroprevalence study in one of the largest slums in CABA and found, three months after the first reported case, a prevalence of 53.4%. Mobility was also analyzed in Buenos Aires City, as a proxy for effectiveness of lockdown measures. For instance, in [12], researchers found a delay of 8 days between changes in mobility and reported cases, while deaths follow cases from 16 to 19 days after.

Beyond the measures imposed by the government at a national level, each city has the autonomy of taking different actions against the disease. Crucial factors such as hospital

capacity, demographic structure, and economic activities, among others, strongly vary between cities. Therefore, local authorities must adapt national guidelines to their own region and determine proper criteria in the decision-making process. For this reason, our study is focused in Mar del Plata (MDP), the main city of the Municipality of General Pueyrredón in Argentina. With this work we aim to provide a key study that will help local governments in decision-making and implementation of mitigation strategies, as well as estimating the medical resources required to face the consequences of such decisions.

The social and demographic structure of the population is generally reflected in heterogeneous contact patterns among individuals, where age is one of the main determinants of these mixing patterns. For instance, children tend to spend more time with children and members of their household; active adults mix with individuals in their workplace; and so forth. For this reason, a disease transmission route may have mixing patterns among individuals of different age [13]. To account for this contact structure, we use census collected data given by national agencies [14]. We divided the population into age groups and compute different contact matrices associated to different settings -household, workplace, school and general community [15,16].

Once we obtained the Mar del Plata network structure, we consider an extension of the compartmental Susceptible-Exposed-Infected-Recovered (SEIR) model [17] -known as SEIRD- to estimate the evolution of an epidemic. Here,  $D$  takes into account the individuals that died as a consequence of the disease. Also, we differentiate between symptomatic and asymptomatic infected individuals, considering different levels of illness severity for symptomatic patients. As in the real-life scenario, some individuals may not require medical attention at all (mild) and only will have to stay for a certain time at home, while others (severe) will require hospitalization [18].

Even though the scientific community all over the world is working relentlessly in the

development of a vaccine, it will take several months to be applied to the majority of the population, therefore, for now, non-pharmaceutical interventions are necessary to prevent the spread of the virus [19–21]. Conversely, measures such as long lasting quarantines also carry serious psychological and economic consequences, that must be considered. Thus, assessing the severity of SARS-CoV-2 and the study of social-distance mitigation strategies are crucial. Related to this topic, Meidan *et al* [22] proposed a novel alternating quarantine strategy (AQ). In this strategy the population is separate into two groups, in which they alternate successively between quarantine and regular activity in a bi-weekly cycle. They found that this measure can be useful as a primary mitigation strategy, with a comparable impact to that of a strict population-wide quarantine. Nevertheless, the weekly relief allowing people an outlet to continue their activity for half of the time may, itself, increase cooperation levels. Indeed, while a complete lock-down is extremely stressful for the individual, the alternating bi-weekly quarantine routine relaxes the burden, and may encourage compliance.

In this research, we propose a different quarantine scenario with time-windows relaxation of activities -such as opening and closing activities by groups- and we are particularly interested in studying the impact of the implementation of tests. In a different manner from previous studies, in our model we use additional states to describe in more realistic way the hospitalized cases, inasmuch as we are especially interested in estimating the medical resources that should be allocated to sick patients. It is important to note that, even though we chose MDP and calibrated the model for COVID-19, our study can be adapted to any region or country where demographic information is available, and for diseases transmitted similarly by contact.

## 2 Model

### 2.1 Compartments

In this work, we use an extension of the SEIR model to study the spread of COVID-19 in MDP. In this model individuals can be assigned to four different compartments, depending on their health status. Susceptible ( $S$ ) individuals are healthy and prone to be infected, becoming exposed ( $E$ ) when this occurs. At the  $E$  stage, individuals have not developed symptoms yet and they are not contagious. With the onset of symptoms, exposed individuals become infected ( $I$ ) and can propagate the disease. Finally, recovered ( $R$ ) individuals have acquired immunity and no longer propagate the disease. One modification we make to this model is the addition of a compartment of deceased ( $D$ ) individuals, which are usually not distinguished from the recovered individuals. Additionally, we include a compartment of asymptomatic ( $A$ ) individuals, taking into account the infected people who show no symptoms but can still propagate the disease (several publications [23–27] have reported the importance of asymptomatic individuals in the transmission of COVID-19).

As we are especially interested in estimating the medical resources that should be allocated to sick individuals, we model their evolution by recognizing different levels of illness severity. On the one hand, some cases develop a mild ( $M$ ) version of the disease. Thus, according to the protocol applied in Argentina, they may not require medical care, but must remain isolated at their homes or in isolation sites prepared for this purpose, until they recover. On the other hand, some individuals develop more serious symptoms and are hospitalized ( $\mathcal{H}$ ) for control. Finally, we divide the hospitalized patients into four categories, based on the fact that the evolution of each type of patient has particular characteristic times and requires different resources from the hospital:

1.  $H$ : those in general beds who will fully recover from the disease,

2.  $H^*$ : those in the intensive care units (ICU) who will fully recover from the disease,
3.  $H^\dagger$ : those in general beds who will die,
4.  $H^{\dagger*}$ : those in the ICU who will die.

Note that we use  $\mathcal{H}$  when referring to all compartments of hospitalized individuals together, as a set. For the different subgroups of  $\mathcal{H}$ , i.e, the  $H$ 's, we use a dagger ( $\dagger$ ) as a notation to mark the compartments that evolve to the compartment  $D$  of deceased individuals, while an asterisk ( $*$ ) denotes the compartments of individuals that make use of intensive care units (ICU).

In Fig 1 we show a flowchart of our model. At the beginning, most of the population starts in the  $S$  compartment. With an effective rate dependent on  $\beta$ , susceptible individuals evolve to the  $E$  compartment, because of the interaction with the infected population. The exposed population becomes infected with rate  $\alpha$ ; a fraction  $\epsilon$  develops symptoms and progresses to the  $I$  compartment, while the remaining goes to the asymptomatic compartment  $A$ . We consider that symptomatic individuals do not immediately become aware of their health state, thus, we include a rate  $\omega$  for the progression of symptomatic infected ( $I$ ) individuals to the  $M$  and  $\mathcal{H}$  compartments. After this, only a fraction  $\zeta$  of  $I$  individuals are hospitalized, while the remaining are isolated at home ( $M$  compartment). These isolated individuals fully recover from the disease with rate  $\gamma^m$ . On the right side of the flow chart we have the four compartments of hospitalized patients, which are differentiated with the presence of superscripts. The population going to these compartments is determined by the values of the corresponding fractions  $\theta, \theta^*, \theta^\dagger$  and  $\theta^{\dagger*}$ . On the other hand, the exit of these compartments is done with different  $\gamma$ -rates, in case the patients recover, or with different  $\delta$ -rates, for fatal cases. Note that patients in the ICU who will recover, i.e., members of the  $H^*$  compartment, first flow to the  $H$  compartment.

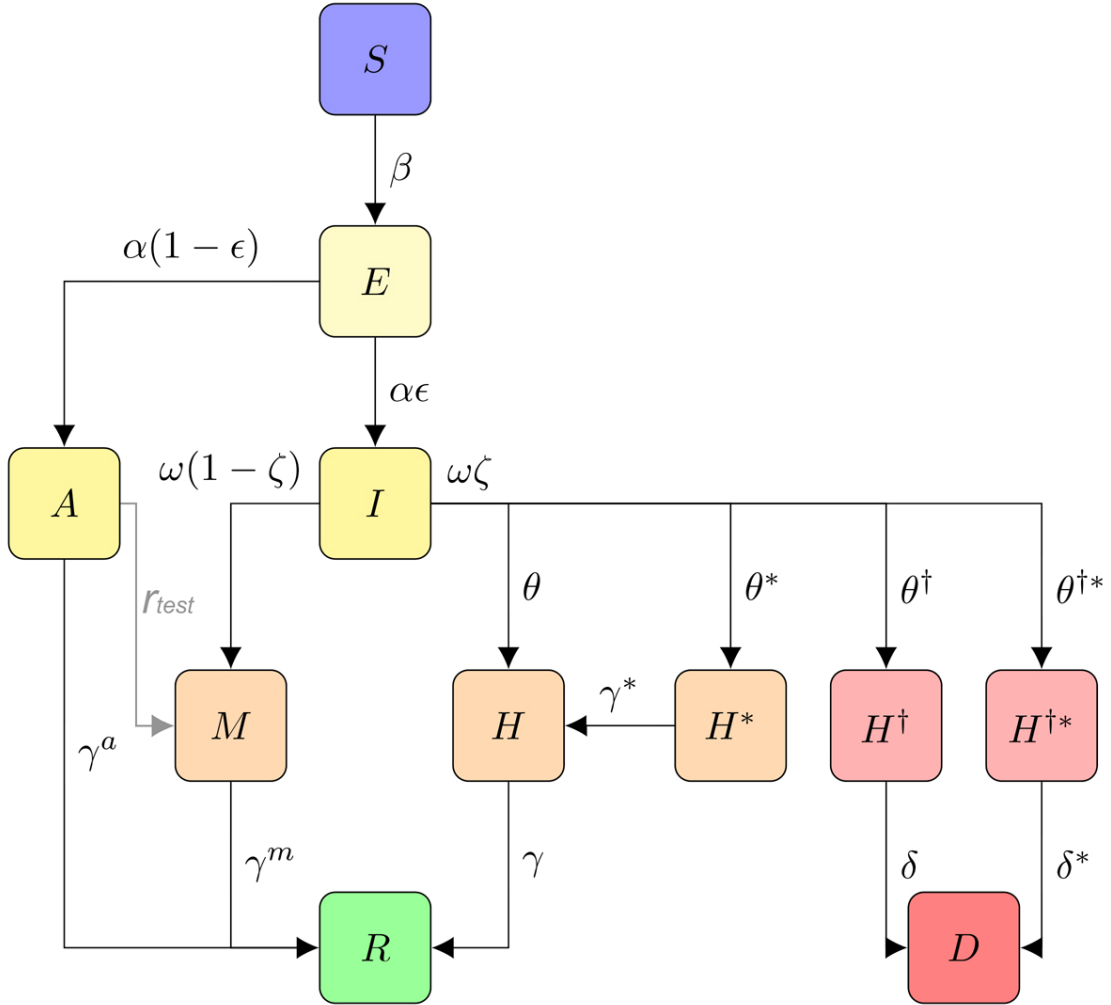


**Fig 1. Flowchart of our epidemic model.** We estimate the initial values of individuals in each compartment by adjusting the curve of deaths in the municipality. The susceptible population  $S$  evolves to the exposed compartment  $E$  with an effective rate dependent on  $\beta$  because of the interaction with symptomatic and asymptomatic infected individuals,  $I$  and  $A$ , respectively. The exposed population becomes infected with rate  $\alpha$ ; a fraction  $\epsilon$  develops symptoms and progresses to the  $I$  compartment, while the remaining goes to the asymptomatic compartment  $A$ . Symptomatic infected individuals pass to one of the compartments among the  $M$  and  $H$  with a rate  $\omega$ . On the right side of the flow chart we have the four hospitalized compartments, which are differentiated with the presence of superscripts. Finally, individuals can end up in one of the two final states, recovered ( $R$ ) or deceased ( $D$ ). Note that the gray arrow from the  $A$  to the  $M$  compartment corresponds to the testing strategy we explain in the Asymptomatic testing subsection.

The choice of multiple  $\mathcal{H}$  compartments ensures that the fractions of patients who fully recover from the disease and those who die are consistent with the values reported in the literature. These fractions are only determined by  $\theta, \theta^*, \theta^\dagger$ , and  $\theta^{\dagger*}$ , and not by the output rates. A summary of the states and parameters can be found in S1 Table and S2 Table.

## 2.2 System of equations

In an effort to better represent the society we are studying, we will divide the population into age groups and incorporate contact matrices [28] to our model. These matrices indicate the mixing patterns between individuals of the population, i.e., the frequency with which people of a certain age interact with each other, and with people from different age groups. This enables us to estimate better the impact over the health system, and the medical resources that will be required. For this matter, we use the census data collected by official organizations [14] and the inferring method developed in [16] to compute the matrices associated with different kinds of social settings: households, workplaces, schools, and general community. For the sake of this work being self-contained, a summary of the inference method can be found in S1 Calculation.

Each age group has its own set of equations describing the evolution of the disease spread, which is indicated by the subscript  $i$ . Note that some parameters are age-dependent while others are not, indicated by the presence or absence of this subscript. The evolution of each group is given by:

$$\frac{dS_i}{dt} = -\mathcal{F}_i(t) S_i, \tag{1}$$

$$\frac{dE_i}{dt} = \mathcal{F}_i(t) S_i - \alpha E_i, \tag{2}$$

$$\frac{dI_i}{dt} = \alpha \epsilon E_i - \omega I_i, \tag{3}$$

$$\frac{dA_i}{dt} = \alpha (1 - \epsilon) E_i - \gamma^a A_i \quad (4)$$

$$\frac{dM_i}{dt} = \omega (1 - \zeta_i) I_i - \gamma^m M_i, \quad (5)$$

$$\frac{dH_i}{dt} = \omega \zeta_i \theta_i I_i + \gamma^* H_i^* - \gamma H_i, \quad (6)$$

$$\frac{dH_i^*}{dt} = \omega \zeta_i \theta_i^* I_i - \gamma^* H_i^*, \quad (7)$$

$$\frac{dH_i^\dagger}{dt} = \omega \zeta_i \theta_i^\dagger I_i - \delta H_i^\dagger, \quad (8)$$

$$\frac{dH_i^{\dagger*}}{dt} = \omega \zeta_i \theta_i^{\dagger*} I_i - \delta^* H_i^{\dagger*}, \quad (9)$$

$$\frac{dR_i}{dt} = \gamma^a A_i + \gamma^m M_i + \gamma H_i, \quad (10)$$

$$\frac{dD_i}{dt} = \delta H_i^\dagger + \delta^* H_i^{\dagger*}, \quad (11)$$

where the force of infection  $\mathcal{F}_i(t)$  is defined by

$$\mathcal{F}_i(t) = \sum_j C_{ij} \frac{\beta (I_j + A_j)}{N_j}, \quad (12)$$

being  $C_{ij}$  the element of the contact matrix which gives the contact frequency between individuals of age  $i$  and  $j$ , and  $N_j$  the total number of individuals of age  $j$ . S1 Table and S2 Table show the parameters of our model and their values. We denote  $\beta$  as  $\beta_{free}$  for the case of free propagation without intervention.

### 2.3 Intervention strategy

In the absence of a vaccine that would prevent the disease from spreading widely, it is of major importance that society implements different non-medical policies to prevent and mitigate the damages that COVID-19 may cause. Being able to estimate the amount of resources that will be needed, as the epidemic progresses, is a key aspect that authorities should seek in order to implement appropriate policies. In this section, we present a

particular intervention strategy that could be helpful in accomplishing a rather controlled progression of COVID-19 in any population, although we focus in MDP, for which we use its census data.

The AQ (alternating quarantine) strategy consists in dividing the population into different groups that face alternate periods of activity/isolation, in terms of socioeconomic activities (education, work, recreation, transportation, etc.). There is one group that it is permanently active (labeled as  $q_0$ ). The remaining population is separated into two equal parts ( $q_1$  and  $q_2$ ), one that is active and in contact with the  $q_0$  group, and one that implements a strict lockdown (these isolated individuals can not propagate the disease). After an established period of time  $\tau$ ,  $q_1$  and  $q_2$  switch places. This parameter will be tuned in order to find the best possible scenario for diminishing the spread of the disease.

For this strategy, we subdivide each compartment  $S_i$ ,  $E_i$ ,  $I_i$  and  $A_i$  into three groups  $q_0$ ,  $q_1$ , and  $q_2$  (the labels represent also the fraction of the population in each group). Thus, adapting Eq. (12) to the case of alternating quarantine, the force of infection for each group must be rewritten as follows:

$$\mathcal{F}_i^{\mathcal{Q}}(t) = \sum_j C_{ij} \frac{\beta^{\mathcal{Q}} (I_j^{\mathcal{Q}} + I_j^{q_0} + A_j^{\mathcal{Q}} + A_j^{q_0})}{N_j},$$

$$\mathcal{F}_i^{q_0}(t) = \mathcal{F}_i^{q_1}(t) + \mathcal{F}_i^{q_2}(t),$$

where  $\mathcal{Q} = \{q_1, q_2\}$ . The rates of infection are given by:

$$\beta^{q_1} = \beta_{free} \Theta \left[ \text{Sin} \left( \frac{\pi t}{\tau} \right) \right],$$

$$\beta^{q_2} = \beta_{free} \left( 1 - \Theta \left[ \text{Sin} \left( \frac{\pi t}{\tau} \right) \right] \right),$$

where  $\Theta(\cdot) \in [0, 1]$  is the Heaviside function, so that  $\beta^{q_1/q_2} \leq \beta_{free}$ , and  $\Theta[\text{Sin}(\frac{\pi t}{\tau})]$  is a periodic square function of period  $2\tau$ . Note that  $\beta^{q_1}$  and  $\beta^{q_2}$  are perfectly out of phase.

## 2.4 Population-wide testing

A very important tool when facing an epidemic outbreak is the diagnostic of sick people [29]. Identifying infected individuals is crucial to attenuate the propagation, because it allows authorities to isolate specific carriers of the disease. Particularly, the detection of asymptomatic infected individuals (compartment  $A$ ) is a difficult task to achieve, since these individuals do not know they are ill and, therefore, do not seek for medical attention. It is extremely important to find and isolate them as quickly as possible. For this reason, along with the AQ strategy, we implement the testing of a part of the asymptomatic individuals, which then flow, with rate  $r_{test}$ , to the compartment  $M$  of mild patients (see Fig 1). As it is a test without contact tracing in the population, susceptible and exposed individuals will also be randomly tested (which will be considered with a negative result and will remain in their compartment). In the same way, symptomatic infected individuals could also be found, who will be admitted to the hospital or isolated, as previously explained about the evolution of this type of individuals. Mathematically, this means replacing in Eqs. (3), (5)-(9)  $\omega$  by  $\omega' = \omega + r_{test}$ . As it is an expensive strategy, we consider that it ceases to be applied when the curve of infected individuals falls below its initial value.

We expect, however, additional measures to be implemented parallel to the AQ strategy and the asymptomatic individuals seeking, to help and reinforce the mitigation capacity of the society against the spread of COVID-19, such as the extended use of face masks, keeping strict hygienic regulations at the workplace, physical distancing and reduction of social gatherings.

## 2.5 ICU capacity

In general, local and national governments make public health decisions based on the projected availability of medical resources, such as ICU capacity, in terms of beds, ventilators, and the specialized workers which operate the equipment and treat the patients [30,31]. The exponential growth of COVID-19 spread may cause a quickly depletion of resources and the saturation of the health system. As a result, an important number of people may not have access to appropriate treatments and could die. Therefore, we consider that a statistical study that explores the evolution of the ICU resources from the health system is of utmost importance. For this reason, we implement a finite number of ICU resources and consider that, when the occupation reaches this limit, the health system is saturated, meaning that new patients that require ICU immediately evolve to the compartment  $D$  of deceased individuals, as long as the system remains saturated. We study particularly the consequences of an overwhelmed health system by looking to the amount of avoidable deaths.

Despite the fact that the local authorities have not reported an official number of available ICU beds [32], we estimate that there are roughly 180 ICU beds in the municipality, and approximately 60 of these beds are available to accommodate COVID-19 patients [33,34].

## 3 Results and discussion

This section will study the effect of a massive testing and AQ strategies applied since September 30, 2020. Note that before this date, the municipality had imposed a mandatory lock-down [35] where many non-essential stores were closed. Fitting our model (see Eqs. (1)-(11)) to the actual data from August 18 to September 30, we obtain that in this period, the effective reproductive number was  $R_0 = 1.5$ , and the effective rate of infection was

$\beta = 3.45$ . To fit  $\beta$ , we integrate our differential equations for different values of  $\beta$  in the interval  $[2.3, 8.0]$  (corresponding to  $R_0 \in [1.0, 3.5]$ ), and then, we choose the optimum value that minimizes the square distance between the predicted number of accumulated deaths and their reported values. Note that we integrate our equations without any strategy to fit our model to the data. The value of  $R_0$  found is notably lower than the reproductive number  $R_0 \approx 2.5$  ( $\beta_{free} = 5.6$ ) that was estimated in previous works [36–38] for a free propagation without any intervention. This result indicates that the municipality’s policies were successful in slowing down the spread of the virus but they also caused a substantial economic cost.

We first study the effect of the AQ on the epidemic spreading for different values of  $\tau$  and  $q_0$ , without implementing the testing strategy ( $r_{test} = 0$ ). To this end, we solve numerically Eqs. (1)-(11) and compute the cumulative number of infected individuals at the final state (when  $I \approx 0$ ), and the height of the peak of active cases under the AQ routine. In Fig 2, these two quantities are plotted as a function of the period  $\tau$ , which ranges from 1 to 14 days. To easily compare the curves of different values of  $q_0$ , we applied a linear transformation on the y-axis to show the y-coordinates in the interval  $[0, 1]$ . As can be seen, the optimal value of  $\tau$  is weakly dependent of the parameter  $q_0$ , with 9 days being the optimum for the accumulated cases (Fig 2A) and 8 days for the peak of active cases (Fig 2B). From here on, we use  $\tau = 7$  in our simulations as it is close to optimal, and in this way, the AQ can be in phase with the standard week. Note that for the particular case  $q_0 = 1$ , the entire population is permanently active, i.e., the AQ strategy is not applied.

In the following, we will study the joint effect of the testing and AQ strategies on the epidemic spreading and how they reduce the pressure on the health system. In Fig 3A we show, a heat map of the peak value of symptomatic infected individuals ( $I$ ) as a function of the fraction of the permanently active population  $q_0$  and the test rate  $r_{test}$ . It can be seen

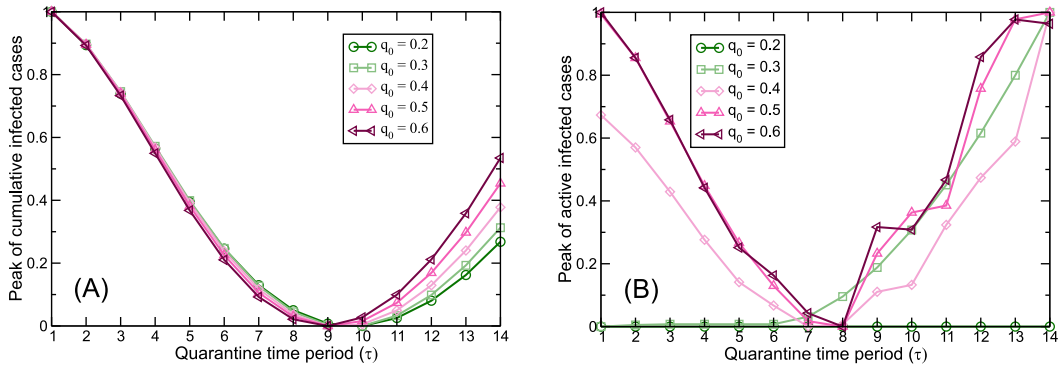


**Fig 2. Optimal value of  $\tau$ .** (A) The accumulated number of infected individuals at the final state and (B) the height of the peak of active cases as a function of  $\tau$  for different values of the parameter  $q_0$ . The values were obtained by solving numerically Eqs. (1)-(11).

that there is a region where the peak coincides with the initial value of infected individuals, implying that the curve of infected cases declines immediately after applying both strategies. In contrast, for higher values of  $q_0$  and lower values of  $r_{test}$ , the peak of infected individuals is up to 10 times higher than the initial condition  $I(t = 0) = I_0$ . This behavior is also shown in Fig 3B, where we plot the time evolution of infected individuals for an increasing value of  $r_{test}$  and  $q_0 = 0.7$ . Recall that the testing strategy is only applied while the number of infected individuals is greater than  $I_0$ , and hence, when  $I(t) < I_0$ , a second wave may hit the municipality. However, for all explored values of  $r_{test}$  and  $q_0$ , we observed that the second wave was either absent or its peak was very close to  $I_0$ . Moreover, for large values of  $r_{test}$ ,  $I(t)$  has a plateau and is slowly decreasing, suggesting that the system is close to a critical point, i.e., the effective reproductive number is  $R_0 \approx 1$ . In the supplementary material (see S1 Fig) we present additional results for the cumulative number of infected individuals.

To further elucidate the effect of the epidemic spreading on the health system, we will compute the minimum number of ICU beds ( $B_{min}$ ) to prevent an overwhelmed healthcare

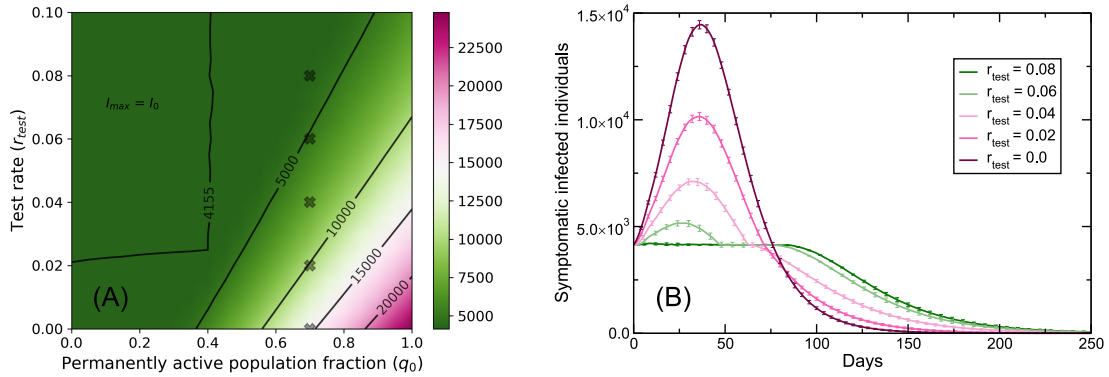


**Fig 3. Evolution of infected individuals.** In (A) we show a heat map of the height of the peak of symptomatic infected individuals  $I_{max}$  in the plane  $q_0$ - $r_{test}$ . The black lines represent isolines and the cross marks serve as a reference for (B). Recall that  $I_0 = I(t = 0)$ . In panel (B), we plot the time evolution of the number of such individuals, where each curve corresponds to a different value of the test rate  $r_{test}$ , with  $q_0 = 0.7$  (these values are marked by cross symbols in panel A). The lines were obtained by solving numerically Eqs. (1)-(11), and the error bars were estimated from 40 stochastic simulations.

system. In order to estimate this magnitude we compute the time evolution of the number of critical patients when there is no restriction on the number of ICU beds, as shown in Fig 4A, for the same values of  $q_0$  and  $r_{test}$  previously used in 3B. Note that the height of the peak of this curve indicates the value of  $B_{min}$  that prevents ICU saturation. In Fig 4B we plot a heat map of  $B_{min}$  and we obtain, as expected, that the two proposed strategies reduce the pressure on the health system, i.e.,  $B_{min}$  decreases for larger values of  $r_{test}$  and smaller values of  $q_0$ . Note that the region to the left side of each isoline of  $B_{min}$  (solid black lines) corresponds to the values of  $q_0$  and  $r_{test}$  where the demand for ICU resources does not exceed the supply  $B_{min}$ . Remarkably, we observed that each line for  $B_{min} < 100$  becomes vertical for a given value of  $q_0$ . Therefore, above this threshold and regardless of the testing strategy level, the demand will overwhelm the ICU supply. In the supplementary material (see S2 Fig), we include a heat map of the period of time in which the health system is

overwhelmed when the number of ICU beds is 60.

In addition, it is also relevant to estimate the total number of tests  $T_{test}$  that the municipality must purchase for a given value of  $r_{test}$  and  $q_0$  because this magnitude can be used to assess the budgetary impact of a massive testing strategy. To estimate this magnitude, we accumulate from our equations, the number of tests used per unit time for 300 days since September 30. The results of this procedure are shown in Fig. 4B as  $T_{test}$ -isolines in the plane  $r_{test}$ - $q_0$  (dashed blue lines). The intersection between the left region of a  $T_{test}$ -isoline and a  $B_{min}$ -isoline indicates the values of  $q_0$  and  $r_{test}$  that meet the budget and ICU capacity. Notably, for a given value of  $q_0$ , the total number of tests saturates as the testing rate  $r_{test}$  increases, which is observed in the figure as a vertical  $T_{test}$ -isoline.

On the other hand, since the ICU bed capacity is a critical bottleneck for the health care system, policymakers must know the total number of deaths  $D_{tot}$  if the ICU capacity is not increased, and also how many deaths would be avoided if the hospitals ensured a minimum number of ICU beds to prevent saturation. In Fig. 4C we show a heat map of  $D_{tot}$  at the final state when the number of ICU beds is 60. In the range of explored values, we observe that decreasing the fraction of permanently active individuals ( $q_0$ ) reduces  $D_{tot}$  more significantly than a higher testing rate  $r_{test}$ . Furthermore, the massive testing strategy has a meaningful effect on  $D_{tot}$  only when  $q_0 > 0.7$ . Besides, we also include in the same figure the isolines of the number of deaths avoided (dashed blue lines) in the scenario where the authorities extend the ICU capacity to prevent an overwhelmed health care system. It can be seen that for the case of a weak AQ strategy (high values of  $q_0$ ) the total number of deaths due to the lack of ICU beds ranges from 250 to 1000 people which corresponds to up to 30% of the total number of deaths.

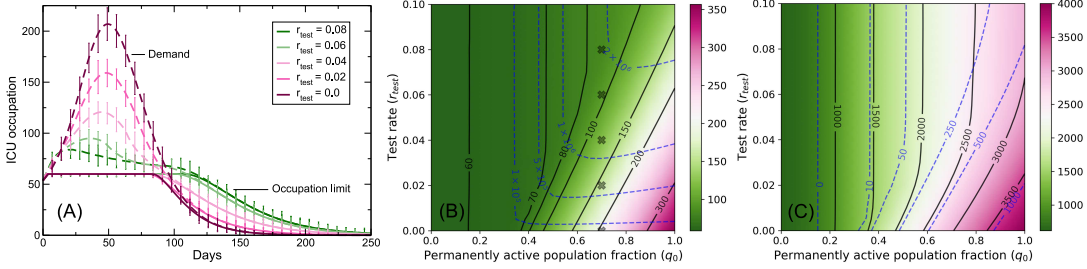


**Fig 4. Impact on the health system.** (A) Time evolution of the ICU occupation when the number of ICU beds is 60 (solid lines) and infinite (dashed lines). Each curve corresponds to a different value of the test rate  $r_{test}$ , with  $q_0 = 0.7$ . The error bars were estimated from 40 stochastic simulations. (B) Heat map showing the minimum number of ICU beds ( $B_{min}$ ) to prevent hospital saturation in the plane of  $r_{test}$  and  $q_0$ . The black lines represent isolines while the cross marks serve as a reference for panel (A). The dashed blue lines correspond to the  $T_{test}$ -isolines (see explanation in the main text). (C) Heat map depicting the total number of deceased individuals ( $D_{tot}$ ) at the final state of the epidemic in the plane  $r_{test}$ - $q_0$  when the total number of ICU beds is 60. The solid black isolines correspond to the total number of deaths ( $D_{tot}$ ) while the dashed blue isolines represent only those deaths due to hospital saturation.

## 4 Conclusion

In this paper we studied a mitigation strategy for COVID-19 spread in Mar del Plata, based on an extended SEIR model, where detected cases are confined and do not propagate the disease. It consists in an alternating quarantine where a portion of the population remains always active, while the rest is divided in two groups and enters a cycle of activity and isolation with period  $2\tau$ . We found that a time-window of  $\tau = 7$  days is the best alternative as it reduces the peak of active and cumulative cases of detected symptomatic patients (a fraction of which eventually die), while it fits with the usual weekly cycle, being easy to implement. Furthermore, we add a testing strategy on the general population, until the number of confirmed cases goes under the initial level. We focused on the pressure over the health system and the death toll that an overwhelmed system may cause. We

found that, given the situation in Mar del Plata as of September 30, extremely low levels of normal circulation would be necessary in order to avoid the saturation of the health system, regardless of the testing rate. The number of ICU beds necessary to prevent saturation increases with the fraction of the population that remains always active, but this number can be shortened by means of an aggressive testing strategy. In the worst case scenario, we estimate that thousands of people may die, but would not if correctly assisted. Therefore, we consider that implementing an alternating quarantine strategy with high testing rates and medium-to-low levels of free circulation is fundamental in order to change the trend of COVID-19 spread in Mar del Plata. Authorities might have to balance testing and equipment costs with mobility levels of the population, in order to arrive at a consistent strategy that people is able to follow, thus, ensuring compliance and reducing the economic, social and psychological effects that long and extended - or the lack of - quarantines produce.

Finally, we emphasize the usefulness of having a model that incorporates the characteristics of society in a specific city, as a tool for local authorities to make informed decisions. This model can be calibrated to study any disease transmitted by direct contact and adapted to other cities using the corresponding census data.

## Supporting information

**S1 Calculation. Inference of contact matrices.** In order to compute the matrix of an arbitrary setting  $\Delta$  we assume that, for an individual  $k$  of age group  $i$  who shares a particular setting  $a^{(k)}$  with other people, on a regular basis, the contact frequency within this setting is homogeneous, i.e., the probability that  $k$  contacts an individual of age group  $j$  is proportional to the number  $a_j^{(k)}$  of these individuals. Therefore, if we denote by  $v_\Delta^{(k)}$  as the total number of people in  $a^{(k)}$ , we can compute this probability as  $a_j^{(k)}/(v_\Delta^{(k)} - 1)$ . Consequently, the frequency of contacts between individuals of age groups  $i$  and  $j$ , in all settings of type  $\Delta$ , is

$$f_{ij}^\Delta = \begin{cases} \frac{1}{n_i^\Delta} \sum_{k=1}^{N_i} \frac{a_j^{(k)} - \delta_{ij}}{v_\Delta^{(k)} - 1} & \text{if } v_\Delta^k > 1, n_i^\Delta > 0, \\ 0 & \text{otherwise} \end{cases},$$

where  $N_i$  is the total number of individuals of age group  $i$  in the entire population, and  $n_i^\Delta$  is the number of individuals of age group  $i$  with nonzero contacts in the setting  $\Delta$ . Note that the Kronecker delta ( $\delta_{ij}$ ) in the numerator avoids counting  $k$  as a self-contact. After computing  $f_{ij}^\Delta$ , the contact matrix associated with setting  $\Delta$  is given by

$$C_{ij}^\Delta = \frac{n_i^\Delta}{N_i} f_{ij}^\Delta.$$

Performing this calculation for households, workplaces, schools and the general community, we obtain a final expression for the contact matrix by taking the weighted sum

$$C_{ij} = \sum_{\Delta} w^\Delta C_{ij}^\Delta,$$

where the weight  $w^\Delta$  represents the proportion of transmission events that take place in setting  $\Delta$ .

In Ref. [16], the authors consider four social settings: households, workplaces, schools, and general community, and estimate the following weights based on empirical data for influenza-like diseases:

$$\begin{aligned} w^{house} &= 0.30, \\ w^{work} &= 0.19, \\ w^{school} &= 0.18, \\ w^{comm} &= 0.33. \end{aligned}$$

In our model with alternating quarantine strategy, we set that the active population has the same weights as in Ref. [16], whereas for the quarantined population we set  $w^{work} = w^{school} = 0$ , and reduce  $w^{comm}$  by a 93.5%. This percentage is based on a 7-day average as of March 29 of Google's mobility data for transit stations and retail & recreation which corresponds to the early stage of the COVID outbreak when the country was in strict quarantine. Thus, the normalized weights for the quarantined population are given by:

$$\begin{aligned} w^{house} &= 0.98, \\ w^{work} &= 0.0, \\ w^{school} &= 0.0, \\ w^{comm} &= 0.02. \end{aligned}$$

Similarly, based on the mobility reported by Google as of August 14 (average of 7 days), we use the following weights to fit the curve of accumulated deaths in General Pueyrredón from August 18 to September 30 (prior to implementing the mitigation strategies):

$$\begin{aligned} w^{house} &= 0.79, \\ w^{work} &= 0.13, \\ w^{school} &= 0.08, \\ w^{comm} &= 0.02. \end{aligned}$$

**S1 Table. Age-independent parameters.** Table describing the age-independent parameters and their values.

Symbol	Description	Value	Reference	Notes
$\beta_{free}$	rate $S \rightarrow I$	5.6	[36–38]	†
$\alpha$	rate $E \rightarrow I$	$1/(5.1-2.0)$	[37, 39–41]	‡
$\omega$	rate $I \rightarrow M, \mathcal{H}$	$1/(4.0+2.0)$	[41, 42]	‡
$\gamma$	rate $H \rightarrow R$	1/8	[13]	
$\gamma^*$	rate $H^* \rightarrow H$	1/10	[13]	
$\gamma^m$	rate $M \rightarrow R$	1/14	[43]	⊘
$\gamma^a$	rate $A \rightarrow R$	1/9.5	[44]	
$\delta$	rate $H^\dagger \rightarrow D$	1/8	[42]	
$\delta^*$	rate $H^{\dagger*} \rightarrow D$	1/11	[42]	

†: These works report the value of  $R_0$  in the stage of free propagation, from which we calculate  $\beta_{free}$  using the next generation matrix method [45].

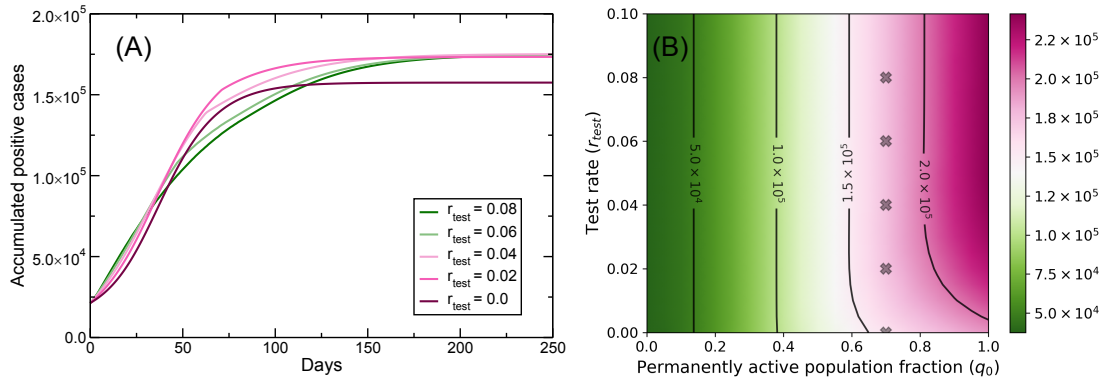
‡: We subtract two days from the time of transition  $E \rightarrow I$  reported in [37, 39, 40], since in [41] the authors estimated that patients are infectious two days before showing symptoms. Therefore, infectious patients also stay two additional days in the community, increasing the time of transition  $I \rightarrow M$  and  $I \rightarrow \mathcal{H}$  reported in [42].

⊘: Health authorities in Argentina require mild patients to remain self-isolated at home, and these cases are reported as recovered after 14 days since their first symptoms appeared.

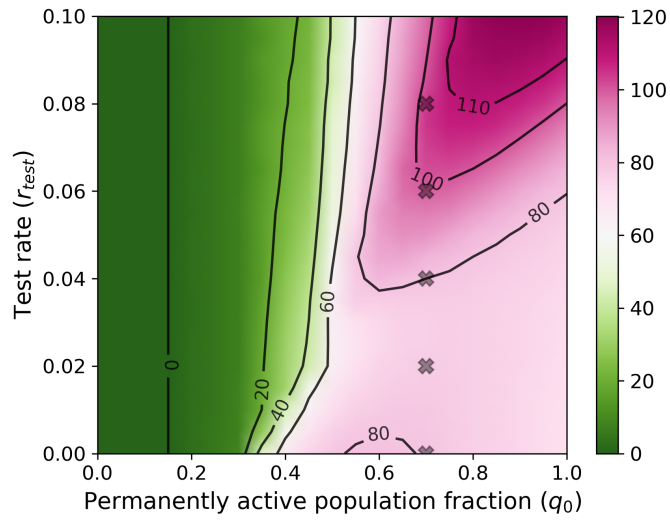
**S2 Table. Age-dependent parameters.** Table describing the age-dependent parameters and their values. The age groups are 5 years wide.

Symbol	Description	Values for Ages [0-4, 5-9, ..., 100-104]	Ref.
$\epsilon$	Proportion of infected individuals that will develop symptoms	1/3, 1/3, 1/3, ..., 1/3, 1, 1, 1	[11, 46] <sup>†</sup>
$\zeta$	Proportion of cases that need hospitalization ( $\mathcal{H}$ )	0.07504484, 0.03803735, 0.02837104, 0.0211873, 0.01936113, 0.02174475, 0.02556259, 0.02665036, 0.03077249, 0.03761504, 0.04842162, 0.0635869, 0.09234972, 0.12900137, 0.17795732, 0.22363486, 0.2618449, 0.28956643, 0.29179373, 0.28364116, 0.1965602	[42]
$\theta$	Proportion of hospitalized patients in general beds who will fully recover	0.93138011, 0.94563427, 0.96491228, 0.9447619, 0.95835351, 0.95063985, 0.94168139, 0.91165612, 0.86417323, 0.81459711, 0.73918075, 0.65684799, 0.53099676, 0.42928786, 0.37042989, 0.31017208, 0.29837518, 0.25360883, 0.25273159, 0.25426357, 0.1625	[42]
$\theta^*$	Proportion of hospitalized patients in ICUs who will fully recover	0.04240555, 0.04448105, 0.02232855, 0.03047619, 0.01985472, 0.019805, 0.02726584, 0.03718354, 0.05068898, 0.05412687, 0.06202268, 0.07073748, 0.06057536, 0.05436309, 0.04901567, 0.03942496, 0.03126539, 0.02462496, 0.02185273, 0.01705426, 0	[42]
$\theta^\dagger$	Proportion of hospitalized patients in general beds who will die	0.00693909, 0.00329489, 0.00637959, 0.01142857, 0.00920097, 0.01279707, 0.01514769, 0.02109705, 0.03617126, 0.05167769, 0.08585975, 0.11180391, 0.18314425, 0.26018054, 0.34491764, 0.42191244, 0.48375185, 0.55165582, 0.59619952, 0.62325581, 0.65	[42]
$\theta^{\dagger*}$	Proportion of hospitalized patients in ICUs who will die	0.01927525, 0.00658979, 0.00637959, 0.01333333, 0.0125908, 0.01675807, 0.01590507, 0.03006329, 0.04896654, 0.07959833, 0.11293682, 0.16061062, 0.22528363, 0.25616851, 0.2356368, 0.22849052, 0.18660758, 0.17011039, 0.12921615, 0.10542636, 0.1875	[42]

<sup>†</sup>: This value was obtained from a seroprevalence study in the city of Buenos Aires, Argentina [11, 46].



**S1 Fig. Effect of the alternating quarantine and the massive testing strategy on the accumulated number of positive cases.** In this figure we present in panel (A) the time evolution of the accumulated number of positive cases, and in panel (B) we show a heat map of these cases at the end of the epidemic in the plane  $r_{test}-q_0$ . The parameters values used for the curves in (A) correspond to those marked by cross marks in (B). Here we define a positive case as either a symptomatic patient or an asymptomatic patient who has been detected by the massive testing strategy. In panel (A) we note that different values of  $r_{test}$  have little effect on the curve for the first 30 days. Similarly, we obtain that for  $t \rightarrow \infty$  and  $r_{test} > 0$ , the strategy has a negligible impact on the final number of positive cases (see panels A and B). As a consequence, these results suggest that it is difficult to assess the impact of such a strategy on the epidemic spreading in the short and long term if the health authorities only report the accumulated number of positive cases, and hence, alternative measures must be considered.



**S2 Fig. Number of days with an overwhelmed health system.** Heat map of the number of days in which hospitals are overwhelmed in the plane  $r_{test} - q_0$  when the number of ICU beds is 60. In the upper right region, this period increases because a higher testing rate delays the extinction of the disease by several weeks, and a weak alternating quarantine ( $q_0 \approx 1$ ) leaves a large proportion of the population exposed to COVID-19.

## Acknowledgments

The authors wish to acknowledge the statistical office that provided the underlying data making this research possible: National Institute of Statistics and Censuses, Argentina. LV, IAP, MT, LDV, CEL and LAB also acknowledge UNMdP (EXA 956/20), CONICET (PIP 00443/2014) and Ministerio de Ciencia, Tecnología e Innovación, Argentina (*Programa de articulación y fortalecimiento federal de las capacidades en ciencia y tecnología COVID-19*) for financial support. We thank Dr. Andrea Perinetti, Dr. Luciano Velázquez, Lic. Laura Lamfre, and Dr. Gustavo Pereyra Irujo for useful discussions.

## References

1. Ministerio de Salud Argentina. ¿Qué medidas está tomando el gobierno?; 2020. <https://www.argentina.gob.ar/coronavirus/medidas-gobierno>, (Accessed: 2020-03-24).
2. Vespignani A, Tian H, Dye C, Smith J, Eggo R, Shrestha M, et al. Modelling COVID-19. *Nature Reviews Physics*. 2020;2:279–281. doi:10.1038/s42254-020-0178-4.
3. Javan E, Fox SJ, Meyers LA. The unseen and pervasive threat of COVID-19 throughout the US. *medRxiv*. 2020;doi:10.1101/2020.04.06.20053561.
4. Wells CR, Sah P, Moghadas SM, Pandey A, Shoukat A, Wang Y, et al. Impact of international travel and border control measures on the global spread of the novel 2019 coronavirus outbreak. *Proceedings of the National Academy of Sciences*. 2020;117(13):7504–7509. doi:10.1073/pnas.2002616117.
5. Oliver N, Lepri B, Sterly H, Lambiotte R, Deletaille S, De Nadai M, et al. Mobile phone data for informing public health actions across the COVID-19 pandemic life cycle. *Science Advances*. 2020;6(23). doi:10.1126/sciadv.abc0764.
6. Ganyani T, Kremer C, Chen D, Torneri A, Faes C, Wallinga J, et al. Estimating the generation interval for COVID-19 based on symptom onset data. *Eurosurveillance*. 2020;25(17):2000257. doi:10.2807/1560-7917.ES.2020.25.17.2000257.
7. Tagliazucchi E, Balenzuela P, Travizano M, Mindlin GB, Mininni PD. Lessons from being challenged by COVID-19. *Chaos, Solitons & Fractals*. 2020;137:109923. doi:10.1016/j.chaos.2020.109923.
8. Jiménez Romero C, Tisnés A, Linares S. Modelo de simulación del COVID-19 basado en agentes. Aplicación al caso argentino. *Posición*. 2020;(3).

9. Neidhöfer G, Neidhöfer C. The effectiveness of school closures and other pre-lockdown COVID-19 mitigation strategies in Argentina, Italy, and South Korea. ZEW-Centre for European Economic Research Discussion Paper. 2020;(20-034).
10. Torrente F, Yoris AE, Low D, Lopez P, Bekinschtein P, Cetkovich M, et al. Sooner than you think: a very early affective reaction to the COVID-19 pandemic and quarantine in Argentina. medRxiv. 2020;doi:10.1101/2020.07.31.20166272.
11. Figar S, Pagotto V, Luna L, Salto J, Manslau MW, Mistchenko A, et al. Community-level SARS-CoV-2 Seroprevalence Survey in urban slum dwellers of Buenos Aires City, Argentina: a participatory research. medRxiv. 2020;doi:10.1101/2020.07.14.20153858.
12. Ahumada H, Espina S, Navajas FH. COVID-19 with uncertain phases: estimation issues with an illustration for Argentina. SSRN. 2020;doi:10.2139/ssrn.3633500.
13. Ferguson N, Laydon D, Nedjati-Gilani G, Imai N, Ainslie K, Baguelin M, et al. Report 9: Impact of non-pharmaceutical interventions (NPIs) to reduce COVID-19 mortality and healthcare demand. Imperial College London. 2020;doi:10.25561/77482.
14. Minnesota Population Center. Integrated Public Use Microdata Series, International: Version 7.2 [dataset]; Minneapolis, MN: IPUMS, 2019. doi:10.18128/D020.V7.2.
15. Mossong J, Hens N, Jit M, Beutels P, Auranen K, Mikolajczyk R, et al. Social Contacts and Mixing Patterns Relevant to the Spread of Infectious Diseases. PLOS Medicine. 2008;5(3):e74. doi:10.1371/journal.pmed.0050074.
16. Fumanelli L, Ajelli M, Manfredi P, Vespignani A, Merler S. Inferring the Structure of Social Contacts from Demographic Data in the Analysis of Infectious Diseases Spread. PLOS Computational Biology. 2012;8(9):e1002673. doi:10.1371/journal.pcbi.1002673.
17. Pastor-Satorras R, Castellano C, Van Mieghem P, Vespignani A. Epidemic processes in complex networks. Reviews of Modern Physics. 2015;87:925–979. doi:10.1103/RevModPhys.87.925.
18. Moghadas SM, Shoukat A, Fitzpatrick MC, Wells CR, Sah P, Pandey A, et al. Projecting hospital utilization during the COVID-19 outbreaks in the United States. Proceedings of the National Academy of Sciences. 2020;117(16):9122–9126. doi:10.1073/pnas.2004064117.
19. Aleta A, Martín-Corral D, Pastore y Piontti A, Ajelli M, Litvinova M, Chinazzi M, et al. Modeling the impact of social distancing, testing, contact tracing and household quarantine on second-wave scenarios of the COVID-19 epidemic. medRxiv. 2020;doi:10.1101/2020.05.06.20092841.

20. Chinazzi M, Davis JT, Ajelli M, Gioannini C, Litvinova M, Merler S, et al. The effect of travel restrictions on the spread of the 2019 novel coronavirus (COVID-19) outbreak. *Science*. 2020;368(6489):395–400. doi:10.1126/science.aba9757.
21. Duque D, Morton DP, Singh B, Du Z, Pasco R, Meyers LA. COVID-19: How to Relax Social Distancing If You Must. *medRxiv*. 2020;doi:10.1101/2020.04.29.20085134.
22. Meidan D, Schulmann N, Cohen R, Haber S, Yaniv E, Sarid R, Barzel B. Alternating quarantine for sustainable epidemic mitigation. *Nature communications*. 2021; 12(1): 1–12. doi:10.1038/s41467-020-20324-8.
23. Gudbjartsson DF, Helgason A, Jonsson H, Magnusson OT, Melsted P, Norddahl GL, et al. Spread of SARS-CoV-2 in the Icelandic Population. *New England Journal of Medicine*. 2020;382(24):2302–2315. doi:10.1056/NEJMoa2006100.
24. Mizumoto K, Kagaya K, Zarebski A, Chowell G. Estimating the asymptomatic proportion of coronavirus disease 2019 (COVID-19) cases on board the Diamond Princess cruise ship, Yokohama, Japan, 2020. *Eurosurveillance*. 2020;25(10):2000180. doi:10.2807/1560-7917.ES.2020.25.10.2000180.
25. Rothe C, Schunk M, Sothmann P, Bretzel G, Froeschl G, Wallrauch C, et al. Transmission of 2019-nCoV Infection from an Asymptomatic Contact in Germany. *New England Journal of Medicine*. 2020;382(10):970–971. doi:10.1056/NEJMc2001468.
26. Nishiura H, Kobayashi T, Miyama T, Suzuki A, Jung SM, Hayashi K, et al. Estimation of the asymptomatic ratio of novel coronavirus infections (COVID-19). *Int J Infect Dis*. 2020;94:154–155. doi:10.1016/j.ijid.2020.03.020.
27. Kimball A, Hatfield K, Arons M, James A, Taylor J, Spicer K, et al. Asymptomatic and Presymptomatic SARS-CoV-2 Infections in Residents of a Long-Term Care Skilled Nursing Facility — King County, Washington, March 2020. *MMWR Morbidity and Mortality Weekly Report*. 2020;69(13):377–381. doi:10.15585/mmwr.mm6913e1.
28. Prem K, Cook AR, Jit M. Projecting social contact matrices in 152 countries using contact surveys and demographic data. *PLOS Computational Biology*. 2017;13(9):e1005697. doi:10.1371/journal.pcbi.1005697.
29. Salathé M, Althaus C, Neher R, Stringhini S, Hodcroft E, Fellay J, et al. COVID-19 epidemic in Switzerland: on the importance of testing, contact tracing and isolation. *Swiss Medical Weekly*. 2020;150:w20225. doi:10.4414/smw.2020.20225.
30. Emanuel EJ, Persad G, Upshur R, Thome B, Parker M, Glickman A, et al. Fair Allocation of Scarce Medical Resources in the Time of Covid-19. *New England Journal of Medicine*. 2020;382(21):2049–2055. doi:10.1056/NEJMs2005114.

31. Wang X, Pasco R, Du Z, Petty M, Fox S, Galvani A, et al. Impact of Social Distancing Measures on Coronavirus Disease Healthcare Demand, Central Texas, USA. *Emerging infectious diseases*. 2020;26(10):2361–2369. doi:10.3201/eid2610.201702.
32. Quédigital. Un nuevo pedido para conocer cuántas camas de terapia intensiva hay en Mar del Plata; 2020. <https://quedigital.com.ar/politica/un-nuevo-pedido-para-conocer-cuantas-camas-de-terapia-intensiva-hay-en-mar-del-plata/>, (Accessed: 2020-10-14).
33. Página12. Mar del Plata: crítica situación de las camas de terapia intensiva; 2020. <https://www.pagina12.com.ar/288336-mar-del-plata-critica-situacion-de-las-camas-de-terapia-inte>, (Accessed: 2020-08-29).
34. Quédigital. Montenegro: “Hoy hay 18 camas libres de terapia, mañana pueden ser 2 y pasado mañana 25”; 2020. <https://quedigital.com.ar/politica/montenegro-mahoy-hay-18-camas-libres-de-terapia-en-mar-del-plata-manana-pueden-ser-2-y-pasado-manana-25/>, (Accessed: 2020-10-07).
35. La Capital. Mar del Plata, en cuarentena: ordenan el cierre de restaurantes, rotiserías, cervecerías y heladerías; 2020. <https://www.lacapitalmdp.com/mar-del-plata-en-cuarentena-ordenan-el-cierre-de-restaurantes-rotiserias-cervecerias-y-heladerias/>, (Accessed: 2020-03-17).
36. Wu JT, Leung K, Leung GM. Nowcasting and forecasting the potential domestic and international spread of the 2019-nCoV outbreak originating in Wuhan, China: a modelling study. *The Lancet*. 2020;395(10225):689–697.
37. Li Q, Guan X, Wu P, Wang X, Zhou L, Tong Y, et al. Early transmission dynamics in Wuhan, China, of novel coronavirus-infected pneumonia. *New England Journal of Medicine*. 2020;.
38. Riou J, Althaus CL. Pattern of early human-to-human transmission of Wuhan 2019 novel coronavirus (2019-nCoV), December 2019 to January 2020. *Eurosurveillance*. 2020;25(4):2000058.
39. Lauer SA, Grantz KH, Bi Q, Jones FK, Zheng Q, Meredith HR, et al. The incubation period of coronavirus disease 2019 (COVID-19) from publicly reported confirmed cases: estimation and application. *Annals of internal medicine*. 2020;172(9):577–582.
40. Linton NM, Kobayashi T, Yang Y, Hayashi K, Akhmetzhanov AR, Jung Sm, et al. Incubation period and other epidemiological characteristics of 2019 novel coronavirus infections with right truncation: a statistical analysis of publicly available case data. *Journal of clinical medicine*. 2020;9(2):538.

41. Byrne AW, McEvoy D, Collins AB, Hunt K, Casey M, Barber A, et al. Inferred duration of infectious period of SARS-CoV-2: rapid scoping review and analysis of available evidence for asymptomatic and symptomatic COVID-19 cases. *BMJ Open*. 2020;10(8). doi:10.1136/bmjopen-2020-039856.
42. Ministerio de Salud Argentina. COVID-19. Casos registrados en la República Argentina [dataset]; 2020. <http://datos.salud.gob.ar/dataset/covid-19-casos-registrados-en-la-republica-argentina>.
43. Ministerio de Justicia y Derechos Humanos. COVID-19 - Aislamiento y distanciamiento social; 2020. <https://www.argentina.gob.ar/justicia/derechofacil/leysimple/covid-19-aislamiento-y-distanciamiento-social>, (Accessed: 2020-09-20).
44. Hu Z, Song C, Xu C, Jin G, Chen Y, Xu X, et al. Clinical characteristics of 24 asymptomatic infections with COVID-19 screened among close contacts in Nanjing, China. *Science China Life Sciences*. 2020;63(5):706–711.
45. Diekmann O, Heesterbeek J, Roberts MG. The construction of next-generation matrices for compartmental epidemic models. *Journal of the Royal Society Interface*. 2010;7(47):873–885.
46. Ministerio de Salud de la Ciudad de Buenos Aires. Coronavirus: el Ministerio de Salud porteño brindó detalles del estudio de seroprevalencia; 2020. <https://www.buenosaires.gob.ar/salud/noticias/coronavirus-el-ministerio-de-salud-porteno-seroprevalencia-buenos-aires>, (Accessed: 2020-11-04).